

Less is More: Compact Matrix Decomposition for Large Sparse Graphs

Jimeng Sun Yinglian Xie Hui Zhang Christos Faloutsos
Carnegie Mellon University
{jimeng,ylxie,hzhang, christos}@cs.cmu.edu

Abstract

Given a large sparse graph, how can we find patterns and anomalies? Several important applications can be modeled as large sparse graphs, e.g., network traffic monitoring, research citation network analysis, social network analysis, and regulatory networks in genes. Low rank decompositions, such as SVD and CUR, are powerful techniques for revealing latent/hidden variables and associated patterns from high dimensional data. However, those methods often ignore the sparsity property of the graph, and hence usually incur too high memory and computational cost to be practical.

We propose a novel method, the *Compact Matrix Decomposition (CMD)*, to compute sparse low rank approximations. CMD dramatically reduces both the computation cost and the space requirements over existing decomposition methods (SVD, CUR). Using CMD as the key building block, we further propose procedures to efficiently construct and analyze dynamic graphs from real-time application data. We provide theoretical guarantee for our methods, and present results on two real, large datasets, one on network flow data (100GB trace of 22K hosts over one month) and one on DBLP (200MB over 25 years).

We show that CMD is often an order of magnitude more efficient than the state of the art (SVD and CUR): it is over *10X faster*, but requires less than *1/10 of the space*, for the same reconstruction accuracy. Finally, we demonstrate how CMD is used for detecting anomalies and monitoring time-evolving graphs, in which it successfully detects worm-like hierarchical scanning patterns in real network data.

1 Introduction

Graphs are used in multiple important applications such as network traffic monitoring, web structure analysis, social network mining, protein interaction study, and scientific computing. Given a large graph, we want to discover patterns and anomalies in spite of the high dimensionality of data. We refer to this challenge as the *static graph mining* problem.

An even more challenging problem is finding patterns in graphs that evolve over time. For example, consider a

network administrator, monitoring the (source, destination) IP flows over time. For a given time window, the traffic information can be represented as a matrix, with all the sources as rows, all the destinations as columns, and the count of exchanged flows as the entries. In this setting, we want to find patterns, summaries, and anomalies for the given window, as well as across multiple such windows. Specifically for these applications that generate huge volume of data with high speed, the method has to be fast, so that it can catch anomalies early on. Closely related questions are how to summarize dynamic graphs, so that they can be efficiently stored, e.g., for historical analysis. We refer to this challenge as the *dynamic graph mining* problem.

The typical way of summarizing and approximating matrices is through transformations, with SVD/PCA [15, 18] and random projections [17] being popular choices. Although all these methods are very successful in general, for large sparse graphs they may require huge amounts of space, exactly because their resulting matrices are not sparse any more.

Large, real graphs are often very sparse. For example, the web graph [20], Internet topology graphs [12], who-trusts-whom social networks [7], along with numerous other real graphs, are all sparse. Recently, Drineas et al. [10] proposed the CUR decomposition method, which partially addresses the loss-of-sparsity issue.

We propose a new method, called *Compact Matrix Decomposition (CMD)*, for generating low-rank matrix approximations. CMD provides provably equivalent decomposition as CUR, but it requires much *less* space and computation time, and hence is *more* efficient.

Moreover, we show that CMD can not only analyze static graphs, but we can also extend it to handle dynamic graphs. Another contribution of our work is exactly a detailed procedure to put CMD into practice, and especially for high-speed applications like internet traffic monitoring, where new traffic matrices are streamed-in in real time.

Overall, our method has the following desirable properties:

- **Fast:** Despite the high dimensionality of large graphs,

the entire mining process is fast, which is especially important for high-volume, streaming applications.

- **Space efficient:** We preserve the sparsity of graphs so that both the intermediate results and the final results fit in memory, even for large graphs that are usually too expensive to mine today.
- **Anomaly detection:** We show how to spot anomalies, that is, rows, columns or time-ticks that suffer from high reconstruction error. A vital step here is our proposed fast method to estimate the reconstruction error of our approximations.

Our work makes contributions to both the theory as well as to the practice of graph mining. From the theoretical viewpoint, we provide the proofs and guarantees about the performance of CMD, both for the static case, as well as for the high-rate extension (Theorem 4.1, Lemma 5.1). From the practical viewpoint, both CMD and its high-rate extension are efficient and effective: our experiments on large, real datasets show that CMD is over *10 times faster* and requires less than *1/10 space* (see Figure 1). We also demonstrate how CMD can help in monitoring and in anomaly detection of time-evolving graphs: As shown in Figure 16 CMD effectively detects real worm-like hierarchical scanning patterns early on.

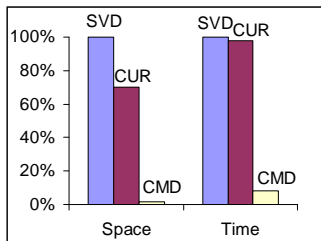


Figure 1: CMD outperforms SVD and CUR significantly in terms of space requirement and computational time. Space and time cost is normalized by the maximum ones (i.e., SVD in both case).

The rest of the paper is organized as follows: Section 2 discusses the related work. Then Section 3 defines our problem more formally. We describe the algorithm and analysis of CMD in Section 4. Section 5 presents the detailed procedures for mining large graphs. Section 6 and Section 7 provide the experimental evaluation and application case study to show the efficiency and applicability of CMD. Finally, we conclude in Section 8.

2 Related Work

Here we discuss related works from three areas: graph mining, numeric analysis and stream mining.

Graph Mining: Graph mining has been a very active area in data mining community. Because of its importance and

expressiveness, various problems are studied under graph mining.

From the modeling viewpoint, Faloutsos et al. [12] have shown the power-law distribution on the Internet graph. Kumar et al. [20] studied the model for web graphs. Leskovec et al. [21] discovered the shrinking diameter phenomena on time-evolving graphs.

From the algorithmic aspect, Yan et al. [26] proposed an algorithm to perform substructure similarity search on graph databases, which is based on the algorithm for classic frequent itemset mining. Cormode and Muthukrishnan [5] proposed streaming algorithms to (1) estimate frequency moments of degrees, (2) find heavy hitter degrees, and (3) compute range sums of degree values on streams of edges of communication graphs, i.e., (source, destination) pairs. In our work, we view graph mining as a matrix decomposition problem and try to approximate the entire graph, which is different to most of the existing graph mining work.

Low rank approximation: SVD has served as a building block for many important applications, such as PCA [18] and LSI [23, 6], and has been used as a compression technique [19]. It has also been applied as correlation detection routine for streaming settings [16, 24]. However, these approaches all implicitly assume dense matrices.

For sparse matrices, the diagonalization and SVD are computed by the iterative methods such as Lanczos algorithm [15]. Recently, Drineas et al. proposed Monte-Carlo approximation algorithms for the standard matrix operations such multiplication [8] and SVD [9], which are two building blocks in their CUR decomposition. CUR has been applied in recommendation system [11], where based on small number of samples about users and products, it can reconstruct the entire user-product relationship.

Streams: Data streams has been extensively studied in recent years. The goal is to process the incoming data efficiently without recomputing from scratch and without buffering much historical data. Two recent surveys [3, 22] have discussed many data streams algorithms, among which we highlight two related techniques: sampling and sketches.

Sampling is a simple and efficient method to deal with large massive datasets. Many sampling algorithms have been proposed in the streaming setting such as reservoir sampling [25], concise samples, and counting samples [14]. These advanced sampling techniques can potentially be plugged into the sparsification module of our framework, although which sampling algorithms to choose highly depends on the application.

“Sketch” is another powerful technique to estimate many important statistics, such as L_p -norm [17, 4], of a semi-infinite stream using a compact structure. “Sketches” achieve dimensionality reduction using random projections as opposed to the best- k rank approximations. Random projections are fast to compute and still preserve the distance

between nodes. However, the projections lead to dense data representations, as oppose to our proposed method.

Finally, Ganti et al. [13] generalize an incremental data mining model to perform change detection on block evolution, where data arrive as a sequence of data blocks. They proposed generic algorithms for maintaining the model and detecting changes when a new block arrives. These two steps are related to our dynamic graph mining.

3 Problem Definition

Without loss of generality, we use the adjacency matrix $\mathbf{A} \in \mathbb{R}^{m \times n}$ to represent a directed graph with weights $G = (V, E, W)$ ¹. Every row or column in \mathbf{A} corresponds to a node in V . We set the value of $\mathbf{A}(i, j)$ to $w(i, j) \in W$ if there is an edge from node $v_i \in V$ to node $v_j \in V$ with weight $w(i, j)$. Otherwise, we set it to zero. For example, in the network traffic matrix case, we could have m (active) sources, n (active) destinations, and for each (source,destination) pair, we record the corresponding count of flows. Note that our definition of the adjacency matrix is more general, because we omit rows or columns that have no entries. It can include both special cases such as bi-partite graphs (rows and columns referring to the different sets of nodes), and traditional graphs (rows and columns referring to the same set of nodes).

Since most graphs from real applications are large but sparse, i.e., the number of edges $|E|$ is roughly linear in the number of nodes $|V|$, we can store them very efficiently using sparse matrix representation by only keeping the nonzero entries. Thus, the space overhead is $O(|V|)$ instead of $O(|V|^2)$.

There are many approaches to extract patterns or structures from a graph given its adjacency matrix. In particular, we consider the patterns as a low dimensional summary of the adjacency matrix. Hence, the goal is to efficiently identify a low dimensional summary while preserving the sparsity of the graph.

More specifically, we formulate the problem as a matrix decomposition problem. The basic question is how to approximate \mathbf{A} as the product of three smaller matrices $\mathbf{C} \in \mathbb{R}^{m \times c}$, $\mathbf{U} \in \mathbb{R}^{c \times r}$, and $\mathbf{R} \in \mathbb{R}^{r \times n}$, such that: (1) $|\mathbf{A} - \mathbf{CUR}|^2$ is small, and (2) \mathbf{C}, \mathbf{U} , and \mathbf{R} can be computed quickly using a small space. More intuitively, we look for a low rank approximation of \mathbf{A} that is both accurate and can be efficiently computed.

With matrix decomposition as our core component, we consider two general class of graph mining problems, depending on the input data:

¹We adopt sparse matrix format where only non-zero entries are stored, whose storage essentially equivalent to adjacency list representation.

²The particular norm does not matter. For simplicity, we use squared Frobenius norm, i.e., $|\mathbf{A}| = \sum_{i,j} \mathbf{A}(i, j)^2$.

Symbol	Description
\mathbf{v}	a vector (lower-case bold)
\mathbf{A}	a matrix (upper-case bold)
\mathbf{A}^T	the transpose of \mathbf{A}
$\mathbf{A}(i, j)$	the entry (i, j) of \mathbf{A}
$\mathbf{A}(i, :)$ or $\mathbf{A}(:, i)$	i -th row or column of \mathbf{A}
$\mathbf{A}(I, :)$ or $\mathbf{A}(:, I)$	sampled rows or columns of \mathbf{A} with id in set I

Table 1: Description of notation.

Static graph mining: Given a sparse matrix $\mathbf{A} \in \mathbb{R}^{m \times n}$, find patterns, outliers, and summarize it. In this case, the input data is a given static graph represented as its adjacency matrix.

Dynamic graph mining: Given timestamped pairs (e.g., source-destination pairs from network traffic, email messages, IM chats), potentially in high volume and high speed, construct graphs, find patterns, outliers, and summaries as they evolve. In other words, the input data are raw event records that need to be pre-processed.

The research questions now are how to sample data and construct matrices (graphs) efficiently? How to leverage the matrix decomposition of the static case, into the mining process? What are the underlying processing modules, and how do they interact with each other? These are all practical questions that require a systematic process. Next we first introduce the computational kernel CMD in Section 4; then we discuss the mining process based on CMD in Section 5.

4 Compact Matrix Decomposition

In this section, we present the Compact Matrix Decomposition (CMD), to decompose large sparse matrices. Such method approximates the input matrix $\mathbf{A} \in \mathbb{R}^{m \times n}$ as a product of three small matrices constructed from sampled columns and rows, while preserving the sparsity of the original \mathbf{A} after decomposition. More formally, it approximates the matrix \mathbf{A} as $\tilde{\mathbf{A}} = \mathbf{C}_s \mathbf{U} \mathbf{R}_s$, where $\mathbf{C}_s \in \mathbb{R}^{m \times c'}$ ($\mathbf{R}_s \in \mathbb{R}^{r' \times n}$) contains $c'(r')$ scaled columns(rows) sampled from \mathbf{A} , and $\mathbf{U} \in \mathbb{R}^{c' \times r'}$ is a small dense matrix which can be computed from \mathbf{C}_s and \mathbf{R}_s . We first describe how to construct the subspace for a given input matrix. We then discuss how to compute its low rank approximation.

4.1 Subspace Construction Since the subspace is spanned by the columns of the matrix, we choose to use sampled columns to represent the subspace.

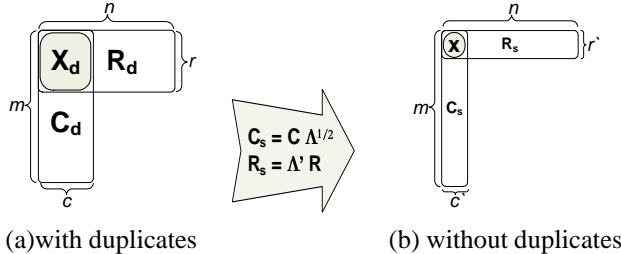
Biased sampling: The key idea for picking the columns is to sample columns with replacement biased towards those ones with higher norms. In other words, the columns with higher entry values will have higher chance to be selected multiple times. Such sampling procedure, used by CUR, is proved to yield an optimal approximation [10]. Figure 2 lists the detailed steps to construct a low dimensional subspace for further approximation. Note that, the biased sampling will bring a lot of duplicated samples. Next we discuss how to

remove them without affecting the accuracy.

-
- Input:** matrix $\mathbf{A} \in \mathbb{R}^{m \times n}$, sample size c
- Output:** $\mathbf{C}_d \in \mathbb{R}^{m \times c}$
1. for $x = 1 : n$ [column distribution]
 2. $P(x) = \sum_i \mathbf{A}(i, x)^2 / \sum_{i,j} \mathbf{A}(i, j)^2$
 3. for $i = 1 : c$ [sample columns]
 4. Pick $j \in 1 : n$ based on distribution $P(x)$
 5. Compute $\mathbf{C}_d(:, i) = \mathbf{A}(:, j) / \sqrt{cP(j)}$
-

Figure 2: Initial subspace construction

Duplicate column removal: CMD carefully removes duplicate columns and rows after sampling, and thus it reduces both the storage space required as well as the computational effort. Intuitively, the directions of those duplicate columns are more important than the other columns. Thus a key step of subspace construction is to scale up the columns that are sampled multiple times while removing the duplicates. Pictorially, we take matrix \mathbf{C}_d , which is the result of Figure 2 (see Figure 3(a)) and turn it into the much narrower matrix \mathbf{C}_s as shown in Figure 3(b), with proper scaling. The method for selecting \mathbf{R}_d and constructing \mathbf{R}_s will be described shortly.



(a) with duplicates (b) without duplicates
Figure 3: Illustration of CUR and CMD

-
- Input:** matrix $\mathbf{A} \in \mathbb{R}^{m \times n}$, sample size c
- Output:** $\mathbf{C}_s \in \mathbb{R}^{m \times c'}$
1. Compute \mathbf{C}_d using the initial subspace construction
 2. Let $\mathbf{C} \in \mathbb{R}^{m \times c'}$ be the unique columns of \mathbf{C}_d
 3. For $i = 1 : c'$
 4. Let u be the number of $\mathbf{C}(:, i)$ in \mathbf{C}_d
 5. Compute $\mathbf{C}_s(:, i) \leftarrow \sqrt{u} \cdot \mathbf{C}(:, i)$
-

Figure 4: CMD subspace construction

Figure 4 shows the algorithm to construct a low dimensional subspace represented with a set of *unique* columns. Each column is selected by sampling the input matrix \mathbf{A} , and then scaling it up based on square root of the number of times it being selected. The resulting subspace also emphasizes the impact of large columns to the same extent as the result in Figure 2. Using the notations in Table 2, we show by 4.1 that the top- k subspaces spanned by \mathbf{C}_d with duplicates and \mathbf{C}_s without duplicates are the same.

Definition	Size
$\mathbf{C} = [\mathbf{C}_1, \dots, \mathbf{C}_{c'}]$	$m \times c'$
$\mathbf{C}_d = \underbrace{[\mathbf{C}_1, \dots, \mathbf{C}_1]}_{d_1}, \dots, \underbrace{[\mathbf{C}_{c'}, \dots, \mathbf{C}_{c'}]}_{d_{c'}}$	$m \times c, c = \sum_i d_i$
$\mathbf{D} = \underbrace{[\mathbf{e}_1, \dots, \mathbf{e}_1]}_{d_1}, \dots, \underbrace{[\mathbf{e}_{c'}, \dots, \mathbf{e}_{c'}]}_{d_{c'}}$	$c' \times c, c = \sum_i d_i$
$\mathbf{\Lambda} = \text{diag}(d_1, \dots, d_{c'})$	$c' \times c'$
$\mathbf{C}_s = [\sqrt{d_1} \mathbf{C}_1, \dots, \sqrt{d_{c'}} \mathbf{C}_{c'}] = \mathbf{C} \mathbf{\Lambda}^{1/2}$	$m \times c'$
$\mathbf{R} = [\mathbf{R}_1, \dots, \mathbf{R}_{r'}]^T$	$r' \times m$
$\mathbf{R}_d = \underbrace{[\mathbf{R}_1, \dots, \mathbf{R}_1]}_{d'_1}, \dots, \underbrace{[\mathbf{R}_{r'}, \dots, \mathbf{R}_{r'}]}_{d'_{r'}}$	$r \times n, r = \sum_i d'_i$
$\mathbf{D}' = \underbrace{[\mathbf{e}_1, \dots, \mathbf{e}_1]}_{d'_1}, \dots, \underbrace{[\mathbf{e}_{r'}, \dots, \mathbf{e}_{r'}]}_{d'_{r'}}$	$r' \times r, r = \sum_i d'_i$
$\mathbf{\Lambda}' = \text{diag}(d'_1, \dots, d'_{r'})$	$r' \times r'$
$\mathbf{R}_s = [d'_1 \mathbf{R}_1, \dots, d'_{r'} \mathbf{R}_{r'}] = \mathbf{\Lambda}' \mathbf{R}$	$r' \times n$

Table 2: Matrix Definition: \mathbf{e}_i is a column vector with all zeros except a one as its i -th element

THEOREM 4.1. (DUPLICATE COLUMNS) *Matrices \mathbf{C}_s and \mathbf{C}_d , defined in Table 2, have the same singular values and left singular vectors.*

Proof. It is easy to see $\mathbf{C}_d = \mathbf{C} \mathbf{D}^T$. Then we have

$$(4.1) \quad \mathbf{C}_d \mathbf{C}_d^T = \mathbf{C} \mathbf{D}^T (\mathbf{C} \mathbf{D}^T)^T = \mathbf{C} \mathbf{D}^T \mathbf{D} \mathbf{C}^T$$

$$(4.2) \quad = \mathbf{C} \mathbf{\Lambda} \mathbf{C}^T = \mathbf{C} \mathbf{\Lambda}^{1/2} \mathbf{\Lambda}^{1/2} \mathbf{C}^T$$

$$(4.3) \quad = \mathbf{C} \mathbf{\Lambda}^{1/2} (\mathbf{C} \mathbf{\Lambda}^{1/2})^T = \mathbf{C}_s \mathbf{C}_s^T$$

where $\mathbf{\Lambda} \in \mathbb{R}^{k \times k}$ is defined in Table 2³.

Now we can diagonalize either the product $\mathbf{C}_d \mathbf{C}_d^T$ or $\mathbf{C}_s \mathbf{C}_s^T$ to find the same singular values and left singular vectors for both \mathbf{C}_d and \mathbf{C}_s .

4.2 Low Rank Approximation The goal is to form an approximation of the original matrix \mathbf{X} using the sampled column \mathbf{C}_s . For clarity, we use \mathbf{C} for \mathbf{C}_s . More specifically, we want to project \mathbf{X} onto the space spanned by \mathbf{C}_s , which can be done as follows:

- project \mathbf{X} onto the span of \mathbf{C}_s ;
- reduce the cost by further duplicate row removal.

Column projection: We first construct the orthonormal basis of \mathbf{C} using SVD (say $\mathbf{C} = \mathbf{U}_C \mathbf{\Sigma}_C \mathbf{V}_C^T$), and then projecting the original matrix into this identified orthonormal basis $\mathbf{U}_C \in \mathbb{R}^{m \times c}$. Since \mathbf{U}_C is usually large and dense, we do not compute the projection of matrix \mathbf{A} directly as $\mathbf{A} \mathbf{U}_C \mathbf{U}_C^T \in \mathbb{R}^{m \times m}$. Instead, we compute a low rank approximation of \mathbf{A} based on the observation that $\mathbf{U}_c = \mathbf{C} \mathbf{V}_C \mathbf{\Sigma}_C^{-1}$, where $\mathbf{C} \in \mathbb{R}^{m \times c}$ is large but sparse, $\mathbf{V}_C \in \mathbb{R}^{c \times k}$ is dense but small, and $\mathbf{\Sigma} \in \mathbb{R}^{k \times k}$ is a small diagonal

³ \mathbf{e}_i is a column vector with all zeros except a one as its i -th element

matrix⁴. Therefore, we have the following:

$$\begin{aligned}\tilde{\mathbf{A}} &= \mathbf{U}_c \mathbf{U}_c^T \mathbf{A} = \mathbf{C} \mathbf{V}_C \boldsymbol{\Sigma}_C^{-1} (\mathbf{C} \mathbf{V}_C \boldsymbol{\Sigma}_C^{-1})^T \mathbf{A} \\ &= \mathbf{C} (\mathbf{V}_C \boldsymbol{\Sigma}_C^{-2} \mathbf{V}_C^T \mathbf{C}^T) \mathbf{A} = \mathbf{C} \mathbf{T} \mathbf{A}\end{aligned}$$

where $\mathbf{T} = (\mathbf{V}_C \boldsymbol{\Sigma}_C^{-2} \mathbf{V}_C^T \mathbf{C}^T) \in \mathbb{R}^{c \times m}$. Although $\mathbf{C} \in \mathbb{R}^{m \times c}$ is sparse, \mathbf{T} is still dense and big. we further optimize the low-rank approximation by reducing the multiplication overhead of two large matrices \mathbf{T} and \mathbf{A} . Specifically, given two matrices \mathbf{A} and \mathbf{B} (assume $\mathbf{A}\mathbf{B}$ is defined), we can sample both columns of \mathbf{A} and rows of \mathbf{B} using the biased sampling algorithm (i.e., biased towards the ones with bigger norms). The selected rows and columns are then scaled accordingly for multiplication. This sampling algorithm brings the same problem as column sampling, i.e., there exist duplicate rows.

Duplicate row removal: CMD removes duplicate rows in multiplication based on 4.2. In our context, CMD samples and scales r' unique rows from \mathbf{A} and extracts the corresponding r' columns from \mathbf{C}^T (last term of \mathbf{T}). Figure 5 shows the details. Line 1-2 computes the distribution; line 3-6 performs the biased sampling and scaling; line 7-10 removes duplicates and rescales properly.

Input: matrix $\mathbf{A} \in \mathbb{R}^{c \times m}$, $\mathbf{B} \in \mathbb{R}^{m \times n}$, sample size r

Output: $\mathbf{C}_R \in \mathbb{R}^{c \times r}$ and $\mathbf{R}_s \in \mathbb{R}^{r \times n}$

1. for $x = 1 : m$ [row distribution of \mathbf{B}]
2. $Q(x) = \sum_i \mathbf{B}(x, i)^2 / \sum_{i, j} \mathbf{B}(i, j)^2$
3. for $i = 1 : r$
4. Pick $j \in 1 : m$ based on distribution $Q(x)$
5. Set $\mathbf{R}_d(i, :) = \mathbf{B}(j, :) / \sqrt{rQ(j)}$
6. Set $\mathbf{C}_R(:, i) = \mathbf{A}(:, j) / \sqrt{rQ(j)}$
7. $\mathbf{R} \in \mathbb{R}^{r' \times n}$ are the unique rows of \mathbf{R}_d
8. for $i = 1 : r'$
9. u is the number of $\mathbf{R}(i, :)$ in \mathbf{R}_d
10. Set $\mathbf{R}_s(i, :) \leftarrow u \cdot \mathbf{R}(i, :)$

Figure 5: ApprMultiplication algorithm

4.2 proves the correctness of the matrix multiplication results after removing the duplicated rows. Note it is important that we use different scaling factors for removing duplicate columns (square root of the number of duplicates) and rows (the exact number of duplicates). Inaccurate scaling factors will incur a huge approximation error.

THEOREM 4.2. (DUPLICATE ROWS) Let I, J be the set of selected rows (with and without duplicates, respectively): $J = \underbrace{[1, \dots, 1]}_{d'_1}, \dots, \underbrace{[r', \dots, r']}_{d'_{r'}}$ and

⁴In our experiment, both \mathbf{V}_C and $\boldsymbol{\Sigma}_C$ have significantly smaller number of entries than \mathbf{A} .

$I = [1, \dots, r']$. Then given $\mathbf{A} \in \mathbb{R}^{m_a \times n_a}$, $\mathbf{B} \in \mathbb{R}^{m_b \times n_b}$ and $\forall i \in I, i \leq \min(n_a, m_b)$, we have

$$\mathbf{A}(:, J) \mathbf{B}(J, :) = \mathbf{A}(:, I) \boldsymbol{\Lambda}' \mathbf{B}(I, :)$$

where $\boldsymbol{\Lambda}' = \text{diag}(d'_1, \dots, d'_{r'})$.

Proof. Denote $\mathbf{X} = \mathbf{A}(:, J) \mathbf{B}(J, :)$ and $\mathbf{Y} = \mathbf{A}(:, I) \boldsymbol{\Lambda}' \mathbf{B}(I, :)$. Then, we have

$$\begin{aligned}\mathbf{X}(i, j) &= \sum_{k \in J} \mathbf{A}(i, k) \mathbf{B}(k, j) \\ &= \sum_{k \in I} d_{i_k} \mathbf{A}(i, k) \mathbf{B}(k, j) = \mathbf{Y}(i, j)\end{aligned}$$

To summarize, Figure 6 lists the steps involved in CMD to perform matrix decomposition for finding low rank approximations.

Input: matrix $\mathbf{A} \in \mathbb{R}^{m \times n}$, sample size c and r

Output: $\mathbf{C} \in \mathbb{R}^{m \times c}$, $\mathbf{U} \in \mathbb{R}^{c \times r}$ and $\mathbf{R} \in \mathbb{R}^{r \times n}$

1. find \mathbf{C} from CMD subspace construction
2. diagonalize $\mathbf{C}^T \mathbf{C}$ to find $\boldsymbol{\Sigma}_C$ and \mathbf{V}_C
3. find \mathbf{C}_R and \mathbf{R} using ApprMultiplication on \mathbf{C}^T and \mathbf{A}
4. $\mathbf{U} = \mathbf{V}_C \boldsymbol{\Sigma}_C^{-2} \mathbf{V}_C^T \mathbf{C}_R$

Figure 6: CMD Low rank decomposition

5 CMD in practice

In this section, we present several practical techniques for mining dynamic graphs using CMD, where applications continuously generate data for graph construction and analysis.

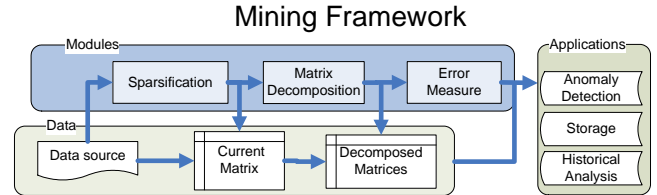


Figure 7: A flowchart for mining large graphs with low rank approximations

Figure 7 shows the flowchart of the whole mining process. The process takes as input data from application, and generates as output mining results represented as low-rank data summaries and approximation errors. The results can be fed into different mining applications such as anomaly detection and historical analysis.

The *data source* is assumed to generate a large volume of real time event records for constructing large graphs (e.g., network traffic monitoring and analysis). Because it is often hard to buffer and process all data that are streamed in, we

propose one more step, namely, *sparsification*, to reduce the incoming data volume by sampling and scaling data to approximate the original full data (Section 5.1).

Given the input data summarized as a *current matrix* \mathbf{A} , the next step is *matrix decomposition* (Section 5.2), which is the core component of the entire flow to compute a lower-rank matrix approximation. Finally, the *error measure* quantifies the quality of the mining result (Section 5.3) as an additional output.

5.1 Sparsification Here we present an algorithm to sparsify input data, focusing on applications that continuously generate data to construct sequences of graphs dynamically. For example, consider a network traffic monitoring system where network flow records are generated in real time. These records are of the form (source, destination, timestamp, #flows). Such traffic data can be used to construct communication graphs periodically (e.g., one graph per hour).

For each time window (e.g., 1pm-2pm), we can incrementally build an adjacency matrix \mathbf{A} by updating its entries as data records are coming in. Each new record triggers an update on an entry (i, j) with a value increase of Δv , i.e., $\mathbf{A}(i, j) = \mathbf{A}(i, j) + \Delta v$.

The key idea to sparsify input data during the above process is to sample updates with a certain probability p , and then scale the sampled matrix by a factor $1/p$ to approximate the true matrix. Figure 8 lists this sparsification algorithm.

Input: update index $(s_1, d_1), \dots, (s_n, d_n)$
sampling probability p
update value Δv

Output: adjacency matrix \mathbf{A}

0. initialize $\mathbf{A} = 0$
1. for $t = 1, \dots, n$
3. if Bernoulli(p)=1 [decide whether to sample]
4. $\mathbf{A}(s_t, d_t) = \mathbf{A}(s_t, d_t) + \Delta v$
5. $\mathbf{A} = \mathbf{A}/p$ [scale up \mathbf{A} by $1/p$]

Figure 8: An example sparsification algorithm

We can further simplify the above process by avoiding doing a Bernoulli draw for every update. Note that the probability of skipping k consecutive updates is $(1 - p)^k p$ (as in the reservoir sampling algorithm [25]). Thus instead of deciding whether to select the current update, we decide how many updates to skip before selecting the next update. After sampling, it is important that we scale up all the entries of \mathbf{A} by $1/p$ in order to approximate the true adjacency matrix (based on all updates).

The approximation error of this sparsification process

can be bounded and estimated as a function of matrix dimensions and the sampling probability p . Specifically, suppose \mathbf{A}^* is the true matrix that is constructed using all updates. For a random matrix \mathbf{A} that approximates \mathbf{A}^* for every of its entries, we can bound the approximation error with a high probability using the following theorem (see [2] for proof):

THEOREM 5.1. (RANDOM MATRIX) *Given a matrix $\mathbf{A}^* \in \mathbb{R}^{m \times n}$, let $\mathbf{A} \in \mathbb{R}^{m \times n}$ be a random matrix such that for all i, j : $\mathbb{E}(\mathbf{A}(i, j)) = \mathbf{A}^*(i, j)$ and $\text{Var}(\mathbf{A}(i, j)) \leq \sigma^2$ and*

$$|\mathbf{A}(i, j) - \mathbf{A}^*(i, j)| \leq \frac{\sigma \sqrt{m+n}}{\log^3(m+n)}$$

For any $m+n \geq 20$, with probability at least $1 - 1/(m+n)$,

$$\|\mathbf{A} - \mathbf{A}^*\|_2 < 7\sigma \sqrt{m+n}$$

With our data sparsification algorithm, it is easy to observe that $\mathbf{A}(i, j)$ follows a binomial distribution with expectation $\mathbf{A}^*(i, j)$ and variance $\mathbf{A}^*(i, j)(1 - p)$. We can thus apply 5.1 to estimate the error bound with a maximum variance $\sigma = (1 - p)\max_{i,j}(\mathbf{A}^*(i, j))$. Each application can choose a desirable sampling probability p based on the estimated error bounds, to trade off between processing overhead and approximation error.

5.2 Matrix Decomposition Once we construct the adjacency matrix $\mathbf{A} \in \mathbb{R}^{m \times n}$, the next step is to compactly summarize it. This is the key component of our process, where various matrix decomposition methods can be applied to the input matrix \mathbf{A} for generating a low-rank approximation. As we mentioned, we consider SVD, CUR and CMD as potential candidates: SVD because it is the traditional, optimal method for low-rank approximation; CUR because it preserves the sparsity property; and CMD because, as we show, it achieves significant performances gains over both previous methods.

5.3 Error Measure The last step of our framework involves measuring the quality of the low rank approximations. An approximation error is useful for certain applications, such as anomaly detection, where a sudden large error may suggest structural changes in the data. A common metric to quantify the error is the sum-square-error (SSE), defined as $\text{SSE} = \sum_{i,j} (\mathbf{A}(i, j) - \tilde{\mathbf{A}}(i, j))^2$. In many cases, a relative SSE ($\text{SSE} / \sum_{i,j} (\mathbf{A}(i, j))^2$), computed as a fraction of the original matrix norm, is more informative because it does not depend on the dataset size.

Direct computation of SSE requires us to calculate the norm of two big matrices, namely, \mathbf{X} and $\mathbf{X} - \tilde{\mathbf{X}}$ which is expensive. We propose an approximation algorithm to

estimate SSE (Figure 9) more efficiently. The intuition is to compute the sum of squared errors using only a subset of the entries. The results are then scaled to obtain the estimated $S\tilde{S}E$.

Input: $\mathbf{A} \in \mathbb{R}^{n \times m}$, $\mathbf{C} \in \mathbb{R}^{m \times c}$, $\mathbf{U} \in \mathbb{R}^{c \times r}$, $\mathbf{R} \in \mathbb{R}^{r \times n}$
sample sizes sr and sc

Output: Approximation error $S\tilde{S}E$

1. rset = sr random numbers from 1:m
2. cset = sc random numbers from 1:n
3. $\tilde{\mathbf{A}}_S = \mathbf{C}(\text{rset}, :) \cdot \mathbf{U} \cdot \mathbf{R}(:, \text{cset})$
4. $\mathbf{A}_S = \mathbf{A}(\text{rset}, \text{cset})$
5. $S\tilde{S}E = \frac{m \cdot n}{sr \cdot sc} \text{SSE}(\mathbf{A}_S, \tilde{\mathbf{A}}_S)$

Figure 9: The algorithm to estimate SSE

With our approximation, the true SSE and the estimated $S\tilde{S}E$ converge to the same value on expectation based on the following lemma⁵. In our experiments (see Section 6.3), this algorithm can achieve small approximation errors with only a small sample size.

LEMMA 5.1. *Given the matrix $\mathbf{A} \in \mathbb{R}^{m \times n}$ and its estimate $\tilde{\mathbf{A}} \in \mathbb{R}^{m \times n}$ such that $\mathbb{E}(\tilde{\mathbf{A}}(i, j)) = \mathbf{A}(i, j)$ and $\text{Var}(\tilde{\mathbf{A}}(i, j)) = \sigma^2$ and a set S of sample entries, then*

$$\mathbb{E}(\text{SSE}) = \mathbb{E}(S\tilde{S}E) = mn\sigma^2$$

where $\text{SSE} = \sum_{i,j} (\mathbf{A}(i, j) - \tilde{\mathbf{A}}(i, j))^2$ and $S\tilde{S}E = \frac{mn}{|S|} \sum_{(i,j) \in S} (\mathbf{A}(i, j) - \tilde{\mathbf{A}}(i, j))^2$

Proof. Straightforward - omitted for brevity.

6 Performance Evaluation

In this section, we evaluate both CMD and our mining framework, using two large datasets with different characteristics. The candidates for comparison include SVD and CUR. The evaluation focuses on 1) space requirement, 2) CPU time, 3) Accuracy estimation cost as well as 4) sparsification effect.

Overall, CMD performs much better than both SVD and CUR as shown in Figure 10⁶.

Next, we first describe our experimental setup including the datasets in Section 6.1. We then compare the space and time requirement of CMD vs. SVD and CUR in Section 6.2. Section 6.3 evaluates the accuracy estimation for CMD and CUR. Finally, Section 6.4 studies the sparsification module.

⁵The variance of SSE and $S\tilde{S}E$ can also be estimated but requires higher moment of $\tilde{\mathbf{A}}$.

⁶These experiments are based on network traffic dataset with accuracy 90%. Note that the estimation cost is not applicable to SVD.

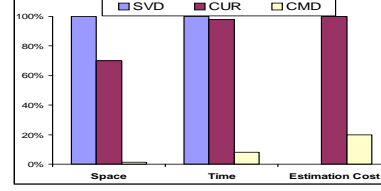


Figure 10: Compared to SVD and CUR, CMD achieves lower space and time requirement as well as fast estimation latency. Note that every thing is normalized by the largest cost in that category when achieving 90% accuracy. e.g., The space requirement of CMD is 1.5% of SVD, while that of CUR is 70%.

6.1 Experimental Setup In this section, we first describe the two datasets; then we define the performance metrics used in the experiment.

data	dimension	$ E $
Network flow	22K-by-22K	12K
DBLP data	428K-by-3.6K	64K

Figure 11: Two datasets

The Network Flow Dataset The traffic trace consists of TCP flow records collected at the backbone router of a class-B university network. Each record in the trace corresponds to a directional TCP flow between two hosts with timestamps indicating when the flow started and finished.

With this traffic trace, we study how the communication patterns between hosts evolve over time, by reading traffic records from the trace, simulating network flows arriving in real time. We use a window size of Δt seconds to construct a source-destination matrix every Δt seconds, where $\Delta t = 3600$ (one hour). For each matrix, the rows and the columns correspond to source and destination IP addresses, respectively, with the value of each entry (i, j) representing the total number of TCP flows (packets) sent from the i -th source to the j -th destination during the corresponding Δt seconds. Because we cannot observe all the flows to or from a non-campus host, we focus on the intranet environment, and consider only campus hosts and intra-campus traffic. The resulting trace has over 0.8 million flows per hour (i.e., sum of all the entries in a matrix) involving 21,837 unique campus hosts.

Figure 12(a) shows an example source-destination matrix constructed using traffic data generated from 10AM to 11AM on 01/06/2005. We observe that the matrix is indeed sparse, with most of the traffic to or from a small set of server-like hosts. The distribution of the entry values is very skewed (a power law distribution) as shown in Figure 12(b). Most of hosts have zero traffic, with only a few of exceptions which were involved with high volumes of traffic (over 10^4 flows during that hour). Given such skewed traffic distribution, we rescale all the non-zero entries by taking the natural

logarithm (actually, $\log(x+1)$, to account for $x=0$), so that the matrix decomposition results will not be dominated by a small number of very large entry values.

Non-linear scaling the values is very important: experiments on the original, bursty data would actually give excellent compression results, but poor anomaly discovery capability: the 2-3 most heavy rows (speakers) and columns (listeners) would dominate the decompositions, and everything else would appear insignificant.

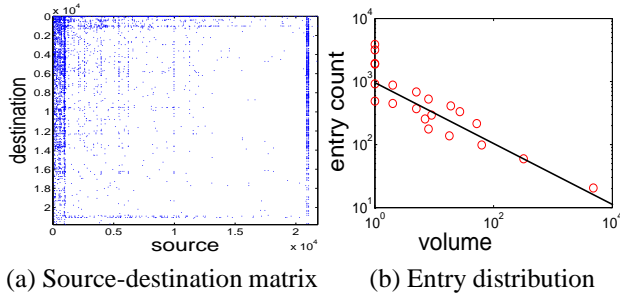


Figure 12: Network Flow: the example source-destination matrix is very sparse but the entry values are skewed.

The DBLP Bibliographic Dataset Based on DBLP data [1], we generate an author-conference graph for every year from year 1980 to 2004 (one graph per year). An edge (a, c) in such a graph indicates that author a has published in conference c during that year. The weight of (a, c) (the entry (a, c) in the matrix \mathbf{A}) is the number of papers a published at conference c during that year. In total, there are 428,398 authors and 3,659 conferences.

The graph for DBLP is less sparse compared with the source-destination traffic matrix. However, we observe that the distribution of the entry values is still skewed, although not as much skewed as the source-destination graph. Intuitively, network traffic is concentrated in a few hosts, but publications in DBLP are more likely to spread out across many different conferences.

Performance Metric We use the following three metrics to quantify the mining performance:

Approximation accuracy: This is the key metric that we use to evaluate the quality of the low-rank matrix approximation output. It is defined as:

$$\text{accuracy} = 1 - \text{relative SSE}$$

Space ratio: We use this metric to quantify the required space usage. It is defined as the ratio of the number of output matrix entries to the number of input matrix entries. So a larger space ratio means more space consumption.

CPU time: We use the CPU time spent in computing the

output matrices as the metric to quantify the computational expense.

All the experiments are performed on the same dedicated server with four 2.4GHz Xeon CPUs and 12GB memory. For each experiment, we repeat it 10 times, and report the mean.

6.2 The Performance of CMD In this section, we compare CMD with SVD and CUR, using static graphs constructed from the two datasets. No sparsification process is required for statically constructed graphs. We vary the target approximation accuracy, and compare the space and CPU time used by the three methods.

Network-Space: We first evaluate the space consumption for three different methods to achieve a given approximation accuracy. Figure 13(1a) shows the space ratio (to the original matrix) as the function of the approximation accuracy for network flow data. Note the Y-axis is in log scale. SVD uses the most amount of space (over 100X larger than the original matrix). CUR uses smaller amount of space than SVD, but it still has huge overhead (over 50X larger than the original space), especially when high accuracy estimation is needed. Among the three methods, CMD uses the least amount of space consistently and achieves over orders of magnitudes space reduction.

The reason that CUR performs much worse for high accuracy estimation is that it has to keep many duplicate columns and rows in order to reach a high accuracy, while CMD decides to keep only unique columns and rows and scale them carefully to retain the accuracy estimation.

Network-Time: In terms of CPU time (see Figure 13(1b)), CMD achieves much more savings than SVD and CUR (e.g., CMD uses less 10% CPU-time compared to SVD and CUR to achieve the same accuracy 90%). There are two reasons: first, CMD compressed sampled rows and columns, and second, no expensive SVD is needed on the entire matrix (graph). CUR is as bad as SVD for high accuracy estimation due to excessive computation cost on duplicate samples. The majority of time spent by CUR is in performing SVD on the sampled columns (see the algorithm in Figure 6)⁷.

DBLP-Space: We observe similar performance trends using the DBLP dataset. CMD requires the least amount of space among the three methods (see Figure 13(1a)). Notice that we do not show the high-accuracy points for SVD, because of its huge memory requirements. Overall, SVD uses more than 2000X more space than the original data, even with a low accuracy (less than 30%). The huge gap between SVD and the other two methods is mainly because: (1) the data distribution of DBLP is not as skewed as that of network

⁷We use LinearTimeCUR algorithm in [10] for all the comparisons. There is another ConstantTimeCUR algorithm proposed in [10], however, the accuracy approximation of it is too low to be useful in practice, which is left out of the comparison.

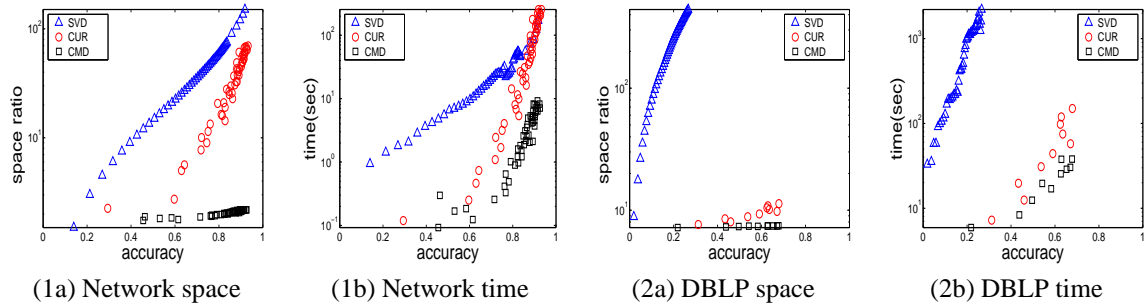


Figure 13: CMD takes the least amount of space and time to decompose the source-destination matrix; the space and time required by CUR increases fast as the accuracy increases due to the duplicated columns and rows.

flow, therefore the low-rank approximation of SVD needs more dimensions to reach the same accuracy, and (2) the dimension for DBLP (428,398) is much bigger than that for network flow (21,837), which implies a much higher cost to store the result for DBLP than for network flow. These results demonstrate the importance of preserving sparsity in the result.

On the other hand, the difference between CUR and CMD in DBLP becomes smaller than that with network flow trace (e.g., CMD is 40% better than CUR for DBLP instead of an order of magnitude better for network.). The reason is that the data distribution is less skewed. There are fewer duplicate samples in CUR.

DBLP-Time: The computational cost of SVD is much higher compared to CMD and CUR (see Figure 13(2b)). This is because the underlying matrix is denser and the dimension of each singular vector is bigger, which explains the high operation cost on the entire graph. CMD, again, has the best performance in CPU time for DBLP data.

6.3 Accuracy Estimation In this section, we evaluate the performance of our accuracy estimation algorithm described in Section 5.3. Note the estimation of relative SSEs is only required with CUR and CMD. For SVD, the SSEs can be computed easily using sum of the singular values.

Using the same source-destination matrix, we plot in Figure 14 (a) both the estimated accuracy and the true accuracy by varying the sample size used for error estimation (i.e., number of columns or rows). For every sample size, we repeat the experiment 10 times with both CUR and CMD, and show all the 20 estimated errors. The targeted low-rank approximation accuracy is set to 90%. We observe that the estimated accuracies (i.e., computed based on the estimated error using $1 - \hat{SSE}$) are close to the true accuracy (*unbiased*), with the variance dropping quickly as the sample size increases (small variance).

The time used for estimating the error is linear to the sample size (see Figure 14). We observe that CMD requires much smaller time to compute the estimated error than CUR (5 times faster). For both methods, the error estimation can

finish within several seconds. As a comparison, it takes longer than 1,000 seconds to compute a true accuracy for the same matrix. Thus for applications that can tolerate a small amount of inaccuracy in accuracy computation, our estimation method provides a solution to dramatically reduce the computation latency.

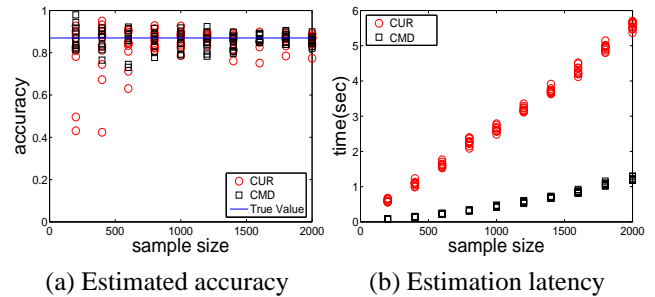


Figure 14: Accuracy Estimation: (a) The estimated accuracy are very close to the true accuracy; (b) Accuracy estimation performs much faster for CMD than CUR

6.4 Robustness to Sparsification We now proceed to evaluate our framework, beginning with the performance of the sparsification module. As described in Figure 8, our proposed sparsification constructs an approximate matrix instead of using the true matrix. Our goal is thus to see how much accuracy we lose using sparsified matrices, compared with using the true matrix constructed from all available data. We use the same source-destination traffic matrix used in Section 6.2. Figure 15 plots the sparsification ratio p vs. accuracy of the final approximation output by the entire framework, using the three different methods, SVD, CUR, and CMD. In other words, the accuracy is computed with respect to the true adjacency matrix constructed with all updates. We also plot the accuracy of the sparsified matrices compared with the true matrices. This provides an upper bound as the best accuracy that could be achieved ideally after sparsification.

Once we get the sparsified matrices, we fix the amount

of space to use for the three different methods. We observe that the accuracy of CMD is very close to the upper bound ideal case. The accuracies achieved by all three methods do not drop much as the sparsification ratio decreases, suggesting the robustness of these methods to missing data. These results indicate that we can dramatically reduce the number of raw event records to sample without affecting the accuracy much.

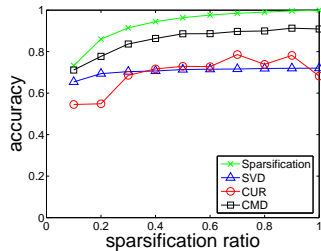


Figure 15: Sparsification: it incurs small performance penalties, for all algorithms.

In summary, CMD consistently outperforms traditional method SVD and the state of art method CUR on all experiments. Next we will illustrate some applications of CMD in practice.

7 Applications and Mining Case Study

In this section, we illustrate how CMD and our framework can be applied in practice using two example applications: (1) anomaly detection on a single matrix (i.e., a *static graph*) and (2) storage, historical analysis, and real-time monitoring of multiple matrices evolving over time (i.e., *dynamic graphs*). For each application, we perform case studies using real data sets.

7.1 Anomaly Detection Given a large static graph, how do we efficiently determine if certain nodes are outliers, that is, which rows or columns are significantly different than the rest? And how do we identify them? In this section, we consider anomaly detection on a static graph, with the goal of finding abnormal rows or columns in the corresponding adjacency matrix. CMD can be easily applied for mining static graphs. We can detect static graph anomalies using the SSE along each row or column as the potential indicators after matrix decomposition.

A real world example is to detect abnormal hosts from a static traffic matrix, which has often been an important but challenging problem for system administrators. Detecting abnormal behavior of host communication patterns can help identify malicious network activities or mis-configuration errors. In this case study, we focus on the static source-destination matrices constructed from network traffic (every column and row corresponds to a source and destination,

Ratio	20%	40%	60%	80%	100%
Source IP	0.9703	0.9830	0.9727	0.8923	0.8700
Destination IP	0.9326	0.8311	0.8040	0.7220	0.6891

Table 3: Network anomaly detection: precision is high for all sparsification ratios (the detection false positive rate = $1 - \text{precision}$).

respectively), and use the SSEs on rows and columns to detect the following two types of anomalies:

Abnormal source hosts: Hosts that send out abnormal traffic, for example, port-scanners, or compromised “zombies”. One example of abnormal source hosts are scanners that send traffic to a large number of different hosts in the system. Scanners are usually hosts that are already compromised by malicious attacks such as worms. Their scanning activities are often associated with further propagating the attack by infecting other hosts. Hence it is important to identify and quarantine these hosts accurately and quickly. We propose to flag a source host as “abnormal”, if its row has a high reconstruction error.

Abnormal destination hosts: Examples include targets of *denial of service* attacks (DoS), or targets of *distributed denial of service* (DDoS). Hosts that receive abnormal traffic. An example abnormal destination host is one that has been under denial of service attacks by receiving a high volume of traffic from a large number of source hosts. Similarly, our criterion is the (column) reconstruction error.

Experimental setup: We randomly pick an adjacency matrix from normal periods with no known attacks. Due to the lack of detailed anomaly information, we manually inject anomalies into the selected matrix using the following method: (1)*Abnormal source hosts:* We randomly select a source host and then set all the corresponding row entries to 1, simulating a scanner host that sends flows to every other host in the network. (2)*Abnormal destination hosts:* Similar to scanner injection, we randomly pick a column and set 90% of the corresponding column entries to 1, assuming the selected host is under denial of service attack from a large number of hosts.

There are two additional input parameters: sparsification ratio and the number of sampled columns and rows. We vary the sparsification ratio from 20% to 100% and set the sampled columns (and rows) to 500.

Performance metrics: We use detection precision as our metric. We sort hosts based their row SSEs and column SSEs, and extract the smallest number of top ranked hosts (say k hosts) that we need to select as suspicious hosts, in order to detect all injected abnormal host (i.e., recall = 100% with no false negatives). Precision thus equals $1/k$, and the false positive rate equals $1 - \text{precision}$.

We inject only one abnormal host each time. And we repeat each experiment 100 times and take the mean.

Results: Table 3(a) and (b) show the precision vs. sparsification ratio for detecting *abnormal source hosts* and *abnormal destination hosts*, respectively. Although the precision remains high for both types of anomaly detection, we achieve a higher precision in detecting abnormal source hosts than detecting the abnormal destinations. One reason is that scanners talk to almost all other hosts while not all hosts will launch DOS attacks to a targeted destination. In other words, there are more abnormal entries for a scanner than for a host under denial of service attack. Most of the false positives are actually from servers and valid scanning hosts, which can be easily removed based on the prior knowledge of the network structure.

Our purpose of this case study is not to present the best algorithm for anomaly detection, but to show the great potential of using efficient matrix decomposition as a new method for anomaly detection. Such approach may achieve similar or better performance than traditional methods but without expensive analysis overhead.

7.2 Time-Evolving Monitoring In this section, we consider the application of monitoring dynamic graphs. Using our proposed process, we can dynamically construct and analyze time-evolving graphs from real-time application data. One usage of the output results is to provide compact storage for historical analysis. In particular, for every timestamp t , we can store only the sampled columns and rows as well as the estimated approximation error $S\tilde{S}E_t$ in the format of a tuple $(C_t, R_t, S\tilde{S}E_t)$.

Furthermore, the approximation error (SSE) is useful for monitoring dynamic graphs, since it gives an indication of how much the global behavior can be captured using the samples. In particular, we can fix the sparsification ratio and the CMD sample size, and then compare the approximation error over time. A timestamp with a large error or a time interval (multiple timestamps) with a large average error implies structural changes in the corresponding graph, and is worth additional investigation.

To make our discussion concrete, we illustrate the application of time-evolving monitoring using both the network traffic matrices and the DBLP matrices.

Network over time: For network traffic, normal host communication patterns in a network should roughly be similar to each other over time. A sudden change of approximation accuracy (i.e., $1 - S\tilde{S}E$) suggests structural changes of communication patterns since the same approximation procedure can no longer keep track of the overall patterns.

Figure 16(b) shows the approximation accuracy over time, using 500 sampled rows and columns without duplicates (out of 21K rows/columns). The overall accuracy remains high. But an unusual accuracy drop occurs during the period from hour 80 to 100. We manually investigate into the trace further, and indeed find the onset of worm-like hierar-

chical scanning activities. For comparison, we also plot the percentage of non-zero matrix entries generated each hour over time in Figure 16(a), which is a standard method for network anomaly detection based on traffic volume or distinct number of connections. Although such statistic is relatively easier to collect, the total number of traffic entries is not always an effective indicator of anomaly. Notice that during the same period of hour 80 to 100, the percentage of non-zero entries is not particularly high. Only when the infectious activity became more prevalent (after hour 100), we can see an increase of the number of non-zero entries. Our framework can thus potentially help detect abnormal events at an earlier stage.

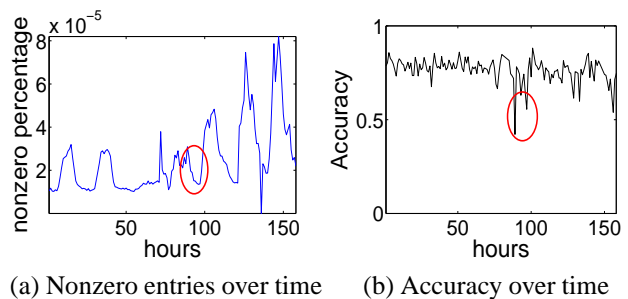


Figure 16: Network flow over time: we can detect anomalies by monitoring the approximation accuracy (b), while traditional method based on traffic volume cannot do (a).

DBLP over time: For the DBLP setting, we monitor the accuracy over the 25 years by sampling 300 conferences (out of 3,659 conferences) and 10 K authors (out of 428K authors) each year. Figure 17(b) shows that the accuracy is high initially, but slowly drops over time. The interpretation is that the number of authors and conferences (nonzero percentage) increases over time (see Figure 17(a)), suggesting that we need to sample more columns and rows to achieve the same high approximation accuracy.

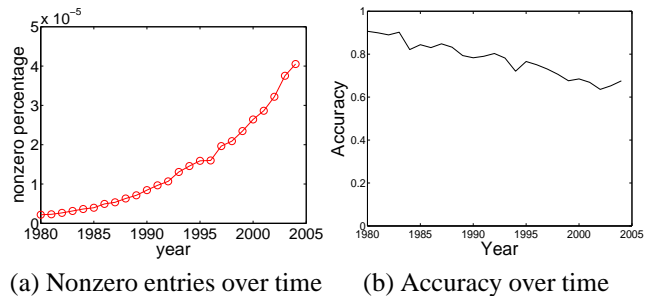


Figure 17: DBLP over time: The approximation accuracy drops slowly as the graphs grow denser.

In summary, our exploration of both applications suggest that CMD has great potential for discovering patterns and anomalies for dynamic graphs too.

8 Conclusion

We studied the problem of efficiently discovering patterns and anomalies from large graphs, like traffic matrices, both in the static case, as well as when they evolve over time. The contributions are the following:

- *New matrix decomposition method:* CMD generates low-rank, sparse matrix approximations. We proved that CMD gives exactly the same accuracy like CUR, but in much less space (Theorem 4.1).
- *High-rate time evolving graphs:* Extension of CMD, with careful sampling, and fast estimation of the reconstruction error, to spot anomalies.
- *Speed and space:* Experiments on several real datasets, one of which is >100Gb of real traffic data, show that CMD achieves up to 10 times less space and less time than the competition.
- *Effectiveness:* CMD found anomalies that were verified by domain experts, like the anomaly in Figure 16

Future work could focus on the time window size: currently, the window size is 1 time-tick. Longer windows might be able to reveal long-term trends, like, e.g., low-rate port-scanners in network intrusion. The choice of the optimal window size is a research challenge.

9 Acknowledgement

We are pleased to acknowledge Petros Drineas and Michael Mahoney for the insightful comments on the work. This material is based upon work supported by the National Science Foundation under Grants No. SENSOR-0329549 EF-0331657 IIS-0326322 IIS-0534205 CNS-0433540 ANI-0331653. This work is also supported in part by the Pennsylvania Infrastructure Technology Alliance (PITA), with funding from Yahoo! research, Intel, NTT and Hewlett-Packard and U.S. Army Research Office contract number DAAD19-02-1-0389. Any opinions, findings, and conclusions or recommendations expressed in this material are those of the author(s) and do not necessarily reflect the views of the National Science Foundation, or other funding parties.

References

- [1] <http://www.informatik.uni-trier.de/ley/db/>.
- [2] D. Achlioptas and F. McSherry. Fast computation of low rank matrix approximations. In *STOC*, 2001.
- [3] B. Babcock, S. Babu, M. Datar, R. Motwani, and J. Widom. Models and issues in data stream systems. In *PODS*, 2002.
- [4] G. Cormode, M. Datar, P. Indyk, and S. Muthukrishnan. Comparing data streams using hamming norms (how to zero in). *TKDE*, 15(3), 2003.
- [5] G. Cormode and S. Muthukrishnan. Space efficient mining of multigraph streams. In *PODS*, 2005.
- [6] S. C. Deerwester, S. T. Dumais, T. K. Landauer, G. W. Furnas, and R. A. Harshman. Indexing by latent semantic analysis. *Journal of the American Society of Information Science*, 41(6):391–407, 1990.
- [7] P. Domingos and M. Richardson. Mining the network value of customers. *KDD*, pages 57–66, 2001.
- [8] P. Drineas, R. Kannan, and M. Mahoney. Fast monte carlo algorithms for matrices i: Approximating matrix multiplication. *SIAM Journal of Computing*, 2005.
- [9] P. Drineas, R. Kannan, and M. Mahoney. Fast monte carlo algorithms for matrices ii: Computing a low rank approximation to a matrix. *SIAM Journal of Computing*, 2005.
- [10] P. Drineas, R. Kannan, and M. Mahoney. Fast monte carlo algorithms for matrices iii: Computing a compressed approximate matrix decomposition. *SIAM Journal of Computing*, 2005.
- [11] P. Drineas, I. Kerenidis, and P. Raghavan. Competitive recommendation systems. In *STOC*, pages 82–90, 2002.
- [12] M. Faloutsos, P. Faloutsos, and C. Faloutsos. On power-law relationships of the internet topology. In *SIGCOMM*, pages 251–262, 1999.
- [13] V. Ganti, J. Gehrke, and R. Ramakrishnan. Mining data streams under block evolution. *SIGKDD Explor. Newsl.*, 3(2), 2002.
- [14] P. B. Gibbons and Y. Matias. New sampling-based summary statistics for improving approximate query answers. In *SIGMOD*, 1998.
- [15] G. H. Golub and C. F. V. Loan. *Matrix Computation*. Johns Hopkins, 3rd edition, 1996.
- [16] S. Guha, D. Gunopulos, and N. Koudas. Correlating synchronous and asynchronous data streams. In *KDD*, 2003.
- [17] P. Indyk. Stable distributions, pseudorandom generators, embeddings and data stream computation. In *FOCS*, 2000.
- [18] I. Jolliffe. *Principal Component Analysis*. Springer, 2002.
- [19] F. Korn, H. V. Jagadish, and C. Faloutsos. Efficiently supporting ad hoc queries in large datasets of time sequences. In *SIGMOD*, pages 289–300, 1997.
- [20] R. Kumar, P. Raghavan, S. Rajagopalan, and A. Tomkins. Extracting large-scale knowledge bases from the web. In *VLDB*, 1999.
- [21] J. Leskovec, J. Kleinberg, and C. Faloutsos. Graphs over time: Densification laws, shrinking diameters and possible explanations. In *SIGKDD*, 2005.
- [22] S. Muthukrishnan. *Data streams: algorithms and applications*, volume 1. Foundations and Trends in Theoretical Computer Science, 2005.
- [23] C. H. Papadimitriou, H. Tamaki, P. Raghavan, and S. Vempala. Latent semantic indexing: A probabilistic analysis. pages 159–168, 1998.
- [24] S. Papadimitriou, J. Sun, and C. Faloutsos. Streaming pattern discovery in multiple time-series. In *VLDB*, 2005.
- [25] J. S. Vitter. Random sampling with a reservoir. *ACM Trans. Math. Software*, 11(1):37–57, 1985.
- [26] X. Yan, P. S. Yu, and J. Han. Substructure similarity search in graph databases. In *SIGMOD*, 2005.